

Research on clock synchronization method of marine controlled source electromagnetic transmitter base on coaxial cable

Zhibin Ren¹, Meng Wang¹, Kai Chen¹, Chentao Wang¹, Runfeng Yu¹

¹China University of Geosciences (Beijing), School of Geophysics and Information Technology, Beijing
CO 100083, China

Correspondence to: Meng Wang (wangmeng@cugb.edu.cn).

Abstract. Marine controlled source electromagnetic (MCSEM) method is widely employed to reveal the electrical structure of shallow media below seafloor. It is an indispensable geophysical means in the exploration of marine oil, gas, natural gas hydrates and seafloor geological structures. The transmitter and receiver in electromagnetic detection equipment need to maintain a high temporal consistency, typically relying on high-stability pulse-per-second (PPS) generated by GPS or BeiDou navigation modules. Coaxial cable is a widely used tow cable, so it is necessary to design a clock synchronization method of marine controlled source electromagnetic transmitter using coaxial cable. This paper proposes a method for synchronizing the internal clock of transmitter with PPS using ship-borne power supply when coaxial cable is used as tow cable. In this method, the ship-borne high-power supply outputs a high-voltage alternating current (AC) signal that is synchronized with 400 Hz signal output from GPS; the coaxial cable transmits AC high-power electrical energy and control commands; the AC signal transmitted via coaxial cable is converted into a stable and continuous 1 Hz signal by step-down, waveform shaping and frequency division for synchronizing the internal time pulses of transmitter. The test result shows that 1 Hz signal obtained by this method has a deviation of approximately 504 ns relative to PPS. This deviation meets MCSEM transmitter's requirement for clock synchronization.

Keywords: marine controlled source electromagnetic, coaxial cable, transmitter, clock synchronization

1 Introduction

Marine controlled source electromagnetic (MCSEM) method is one of the methods in exploration of seafloor natural gas hydrates (Edwards and Chave, 1986; Cox et al., 1986). It is an indispensable geophysical means in the exploration of marine oil, gas, natural gas hydrates and seafloor geological structures (Constable and Srnka, 2007; Constable, 2010). In MCSEM method, the synchronization of internal clocks between transmitter and receiver is an very important issue (Wang et al., 2015b; Meng et al., 2009). Electromagnetic data processing and interpretation depend on synchronization between transmitter and receiver (Qiu et al., 2020). MCSEM transmitter and receiver are separated from each other (Chen et al., 2012; Chen et al., 2020), and they are not connected by any cable. Therefore, Pulse-Per-Second (PPS) signal output from GPS is used as a common synchronization signal to synchronize the internal clock of transmitter and receiver.

The tow cables commonly used in MCSEM transmission systems are photoelectric composite cables and coaxial cables. The transmitter's clock synchronization method varies based on the type of tow cable. When using coaxial cable as tow cable, clock synchronization can be achieved by controlling power supply output or transmitting PPS to transmitter before it is submerged. As an example, SUESI-500 transmitter of Scripps Institution of Oceanography uses a standard UNOLS 0.680 inch

删除[Zhibin Ren]: used

删除[Zhibin Ren [2]]: the

删除[Zhibin Ren [2]]: and

删除[Zhibin Ren [2]]: exploration

删除[Zhibin Ren [2]]: usually using

删除[Zhibin Ren [2]]: as a synchronization signal

删除[Zhibin Ren]: s

删除[Zhibin Ren [2]]: the

删除[Zhibin Ren [2]]: about

删除[Zhibin Ren [2]]: the

删除[Zhibin Ren [2]]: the need of

删除[Zhibin Ren [2]]: and

删除[Zhibin Ren [2]]: exploration

删除[Zhibin Ren [2]]: the

删除[Zhibin Ren [2]]: of

删除[Zhibin Ren [2]]: the

删除[Zhibin Ren [2]]: the

删除[Zhibin Ren [2]]: the

删除[Zhibin Ren [2]]: The

删除[Zhibin Ren [2]]: commonly used

删除[Zhibin Ren [2]]: for

删除[Zhibin Ren [2]]: a

删除[Zhibin Ren [2]]: the

(17.27 mm) coaxial cable as tow cable. They use a 400 Hz output from a GPS clock to generate a 400 Hz sine wave of variable amplitude to control power supply (Constable, 2013; Constable, 2006). **The clock information in power signal serves as a reference for clock-related operations within transmitter.** SUESI-500 transmitter's frequency control signals is generated based on 400 Hz signal. When using photoelectric composite cable as tow cable, clock synchronization can be achieved by transmitting PPS through one channel of optical fiber. For example, the transmitter of China University of Geosciences (Beijing) uses a 32.8 mm photoelectric composite cable as tow cable, and its clock synchronization is achieved by transmitting PPS and GPS time through optical fiber (Wang et al., 2021). However, the cost of photoelectric composite cable is high and generally only large scientific research ships can be equipped. In order to enable MCSEM transmitters work on **a wider variety of ships**, using coaxial cable is necessary. **Compared to photoelectric composite cable**, coaxial cable has only one message channel and can't be assigned a separate channel to transmit PPS. The coaxial cable **can** transmit data and commands **using power line communication**, but **its** delay is unstable. If PPS is transmitted via coaxial cable, it will have a large deviation. Consequently, how to use coaxial cable to synchronize internal clock of MCSEM transmitter is a challenging problem. This paper proposes a clock synchronization method of MCSEM transmitter based on coaxial cable. In this method, the sinusoidal signal from power supply is synchronized with 400 Hz square wave signal from GPS. **Then the sinusoidal power signal transmitted to underwater transmitter is converted into a stable and continuous 1 Hz square wave signal by step-down, waveform shaping and frequency division. The final 1 Hz square wave signal is as the synchronization signal for transmitter's internal clock.**

2 Clock synchronization based on coaxial cable

In this paper, the tow cable used is coaxial cable. This coaxial cable not only transmits electrical energy but also functions as a communication link between deck monitoring terminal and underwater transmitter. Communication is achieved through power line communication technology (Ferreira et al., 2001; Amuta et al., 2020; Kaddoum and Tadayon, 2016). The power transmitted through coaxial cable is a 400 Hz sinusoidal waveform.

Fig.1 illustrates the schematic diagram of MCSEM transmission system, which is based on coaxial cable. The ship is equipped with an instrument control room used to house **personal computer (PC)** and deck monitoring terminal. The deck monitoring terminal is connected to the ship-borne high-power supply, allowing it to control power on/off functions and communication with underwater transmitter. **It** also receives GPS time messages and PPS for clock synchronization. The ship-borne high-power supply generates 0~3000 V, 400 Hz **alternating current (AC)** electricity to power underwater transmitter (Wang et al., 2017b). In addition to transmitting electrical energy, the coaxial cable also transmits commands to underwater transmitter **by power line communication**. The underwater transmitter consists of two main components: a transmission chamber and a control chamber. The transmission chamber **contains** step-down, rectification and inverter units, which transmit high power electromagnetic waves to the seafloor (Wang et al., 2015a). The control chamber contains control circuit **of** entire transmitter, allowing it to transmit frequency-switching signals to control high-current transmission and monitor transmitter's state parameters. The transmitter is also equipped with auxiliary tools such as an altimeter and an attitude module to measure safety-related parameters during underwater towing. **Behind the transmitter, two** electrodes are towed, with a tail fin attached to the electrodes to stabilize their orientation (Wang et al., 2013; Wang et al., 2017a; Liu et al., 2012).

删除[Zhibin Ren [2]]: the
删除[Zhibin Ren [2]]: the
删除[Zhibin Ren [2]]: the
删除[Zhibin Ren]: GPS time provided by the power sign
删除[Zhibin Ren [2]]: a
删除[Zhibin Ren [2]]: the
删除[Zhibin Ren [2]]: the
删除[Zhibin Ren [2]]: the
删除[Zhibin Ren [2]]: more
删除[Zhibin Ren [2]]: However
删除[Zhibin Ren [2]]: compared to photoelectric compo
删除[Zhibin Ren [2]]: uses power line communication to
删除[Zhibin Ren [2]]: signal
删除[Zhibin Ren [2]]: the
删除[Zhibin Ren [2]]: the
删除[Zhibin Ren]: ;
删除[Zhibin Ren]: T
删除[Zhibin Ren]: he
删除[Zhibin Ren [2]]: the
删除[Zhibin Ren [2]]: Finally
删除[Zhibin Ren]: The
删除[Zhibin Ren [2]]: the
删除[Zhibin Ren [2]]: the
删除[Zhibin Ren [2]]: a
删除[Zhibin Ren [2]]: the
删除[Zhibin Ren]: , utilizing a differential chaos shift key
删除[Zhibin Ren [2]]: the
删除[Zhibin Ren [2]]: Fig.1 illustrates the structure of th
删除[Zhibin Ren [2]]: the
删除[Zhibin Ren [2]]: a
删除[Zhibin Ren [2]]: the
删除[Zhibin Ren [2]]: facilitating
删除[Zhibin Ren [2]]: the
删除[Zhibin Ren [2]]: The deck monitoring terminal

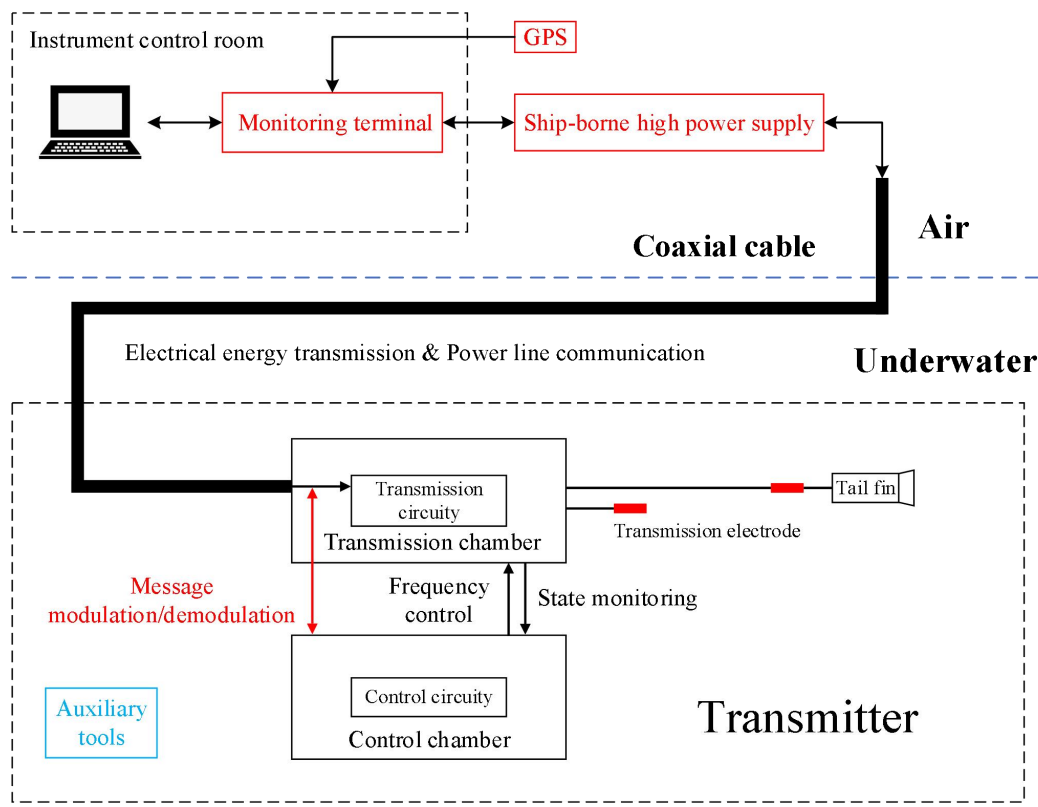


Fig.1 The schematic diagram of MCSEM transmission system based on coaxial cable.

Fig.2 illustrates the synchronization signal flow based on coaxial cable. The GPS module features a TIMEPULSE pin that can be configured to output a 400 Hz square wave, with its rising edges precisely aligned with PPS at integer seconds. The 400 Hz square wave is transmitted to the ship-borne high-power supply through deck terminal as a synchronization signal. To prevent interference from high-power supply, the signal between deck monitoring terminal and power supply is transmitted via an isolated RS485 bus. The 400 Hz sinusoidal signal generated by high-power supply is transmitted to underwater transmitter through coaxial cable, where it is converted to a sinusoidal signal in the range of 0~22 V by two transformers. The signal processing unit in transmitter's control circuit processes the 0~22 V sinusoidal signal and generates a 1 Hz square wave as the synchronization signal for control circuit. The rising edges of 1 Hz square wave are aligned with the rising edges of PPS.

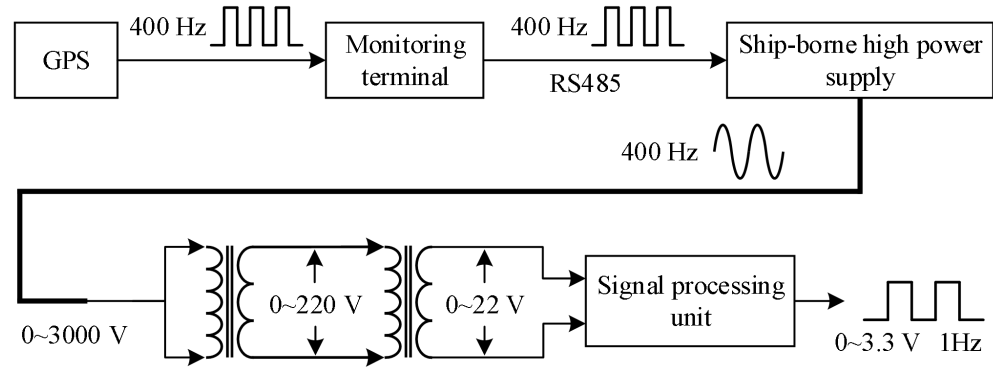


Fig.2 The flow diagram of synchronization signal.

删除[Zhibin Ren [2]]: a
 删除[Zhibin Ren [2]]: the
 删除[Zhibin Ren [2]]: The deck monitoring terminal contains a signal follower that receive 400 Hz square wave from the GPS and transmits it to the ship-borne high-power supply. The 400 Hz AC output from the power supply is synchronized with the 400 Hz square wave.
 删除[Zhibin Ren [2]]: the
 删除[Zhibin Ren [2]]: the

删除[Zhibin Ren [2]]: presents

删除[Zhibin Ren [2]]: the

删除[Zhibin Ren [2]]: facilitates

删除[Zhibin Ren [2]]: the

删除[Zhibin Ren [2]]: output

删除[Zhibin Ren [2]]: the

删除[Zhibin Ren [2]]: the

删除[Zhibin Ren [2]]: power

删除[Zhibin Ren [2]]: the

删除[Zhibin Ren [2]]: synchronization signal access

删除[Zhibin Ren [2]]: It outputs a synchronized sinusoid 

删除[Zhibin Ren [2]]: the

删除[Zhibin Ren [2]]: the

删除[Zhibin Ren [2]]: the

删除[Zhibin Ren [2]]: the

删除[Zhibin Ren [2]]: communication

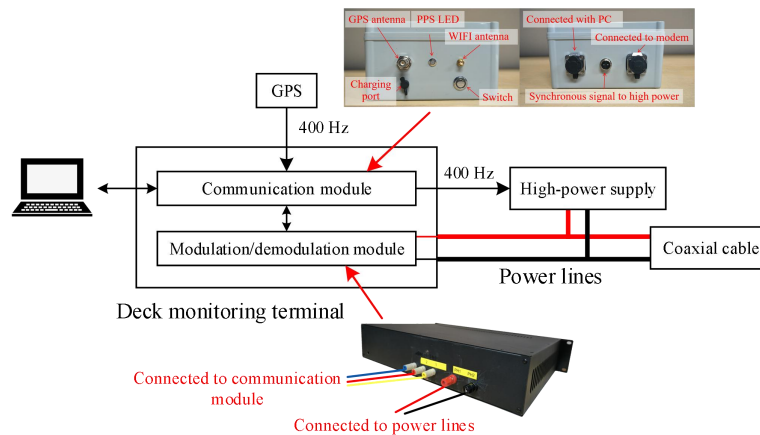
删除[Zhibin Ren [2]]: Another TIMEPULSE pin on the GPS

删除[Zhibin Ren [2]]: the

100 3 Hardware design of clock synchronization method based on coaxial cable

101 3.1 Deck monitoring terminal

102 Fig.3 shows the block diagram of deck monitoring terminal. The deck monitoring terminal comprises a
103 communication module and a coaxial cable modulation/demodulation module (modem). The
104 communication module is responsible for interaction between monitoring software on PC and
105 transmitter. A signal follower within communication module receives 400 Hz signal from GPS and
106 relays it to high power supply as a synchronization signal. The coaxial cable modem modulates
107 messages sent by PC onto two power lines of coaxial cable and demodulates messages returned by
108 transmitter through coaxial cable.



109 **Fig.3** The block diagram of deck monitoring terminal.

109

110

111

112 3.2 High-power supply output synchronized with GPS

113 The high-power supply is designed with a function to accept external synchronization signals. Both the
114 underwater transformers of transmitter and ship-borne high-power supply operate at a frequency of 400
115 Hz. Accordingly, the TIMEPULSE pin of GPS is configured to output a 400 Hz signal and is
116 connected to high-power supply via a RS485 module. This RS485 module will introduce a certain
117 delay. Fig.4 shows the comparison of PPS before and after RS485 transmission. It is observed that the
118 delay introduced by RS485 is less than 50 ns. The power supply output voltage is set to 20 V. The
119 TIMEPULSE pin on another GPS is configured to output a 1 Hz signal, which is monitored alongside
120 the power supply output. Fig.5 shows the synchronized output signal waveform of power supply. It can
121 be observed that the zero phase of power supply output signal is aligned with the rising edge of PPS.
122 After continuous observation, the 400 Hz sinusoidal signal output from power supply remains stable
123 relative to the rising edges position of PPS. This synchronization of power supply output is effective,
124 and forms the foundation of entire clock synchronization method.

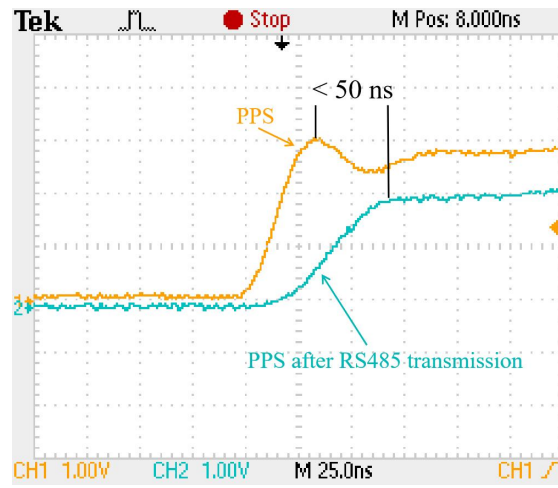


Fig.4 The comparison of PPS before and after RS485 transmission.

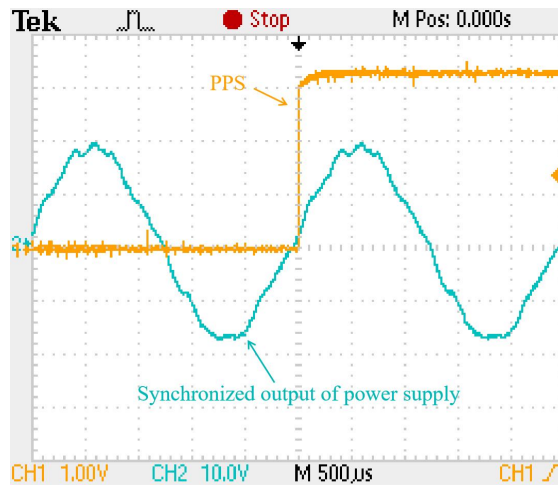


Fig.5 The synchronized output signal waveform of power supply.

3.3 Signal processing unit

The 400 Hz sinusoidal signal output from high-power supply is transmitted to transmitter via a coaxial cable. Then it passes through two transformers and is converted into a sinusoidal wave with an amplitude ranging from 0 to 24 V. This signal is converted into 1 Hz square wave with an amplitude of 0 to 3.3 V by signal processing circuit. Fig.6 shows the hardware of signal processing unit.



Fig.6 The hardware of signal processing unit.

删除[Zhibin Ren [2]]: the
 删除[Zhibin Ren [2]]: the
 删除[Zhibin Ren [2]]: I
 删除[Zhibin Ren [2]]: then
 删除[Zhibin Ren [2]]: 1
 删除[Zhibin Ren [2]]: the

125
126
127

128
129
130

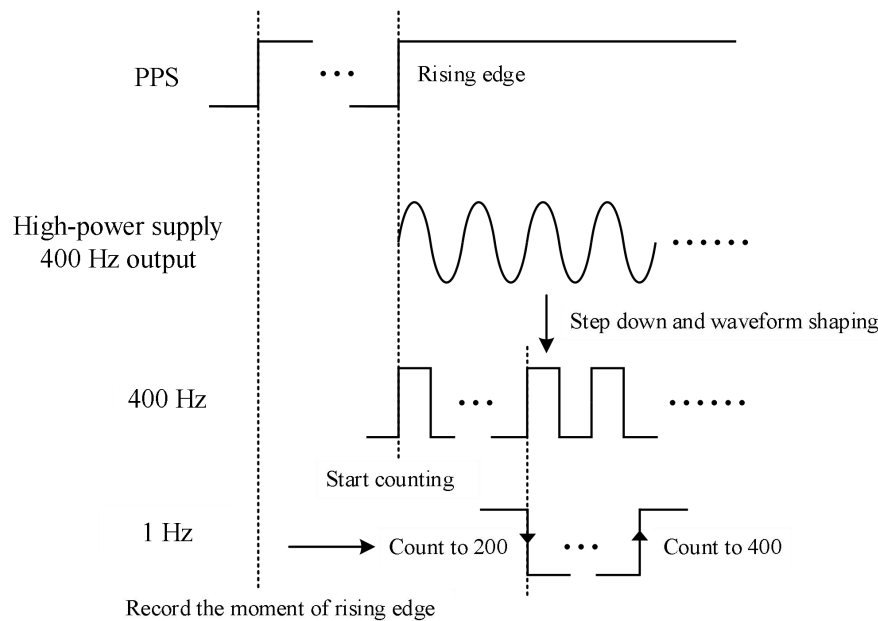
131
132
133
134
135

136
137

138

139 The 400 Hz sinusoidal wave, ranging from 0 to 24 V, is first processed by a common-mode filter to
140 eliminate noise. A protective circuit, consisting of gas discharge tubes (GDT) and transient voltage
141 suppression (TVS) diodes, surrounds common-mode filter circuit to prevent over-voltage and protect
142 subsequent stages. After filtering, the sinusoidal wave is processed through a rectification unit, which
143 converts it into a 0~3.3 V, 400 Hz square wave signal. This rectification unit comprises an optical
144 coupler and an operational amplifier, which rectifies signal, isolates input from output, and protects
145 following operational circuits from sudden variations in the input signal. The square wave signal from
146 rectifier is then processed by the operation unit of underwater signal processing system, which
147 generates a 1 Hz square wave using a pulse counting method. The core of operation unit is a complex
148 programmable logic device (CPLD), which outputs one rising edge for every 400 counted rising edges
149 of 400 Hz square wave. The 1 Hz square wave output by CPLD operation unit is the final
150 synchronization signal transmitted to control circuit.

151 To align the rising edges of 1 Hz square wave with the rising edges of PPS, CPLD module records the
152 exact moment of PPS rising edges. The 1 Hz square wave is aligned with PPS only when CPLD begins
153 counting 400 Hz square wave at the moment of a certain PPS rising edge. Therefore, before
154 submerging transmitter, an external GPS module is connected to it. Once CPLD records the timing of
155 PPS rising edges, it generates an internal 1 Hz signal synchronized with PPS. Afterward, the external
156 GPS module is removed, and power supply is activated. CPLD module initially sets output pin to low
157 and then raises it high upon detecting the first rising edge of internally generated 1 Hz signal, as
158 illustrated in Fig.7. After this, when the rising edge count of 400 Hz signal reaches 200, output pin is
159 set to low, generating a falling edge; when the count of 400 Hz signal reaches 400, output pin is set to
160 high, generating a rising edge and resetting counter for next cycle. The clock synchronization of entire
161 transmitter system depends on the rising edges of PPS, which must be generated with accuracy and
162 stability. Therefore, this method of counting rising edges of 400 Hz signal directly to 400 ensures
163 precise generation of these rising edges.



164

165 **Fig.7 The schematic diagram of 1Hz synchronized signal generation.**

166

删除[Zhibin Ren [2]]: ,

删除[Zhibin Ren [2]]: the

删除[Zhibin Ren [2]]: from

删除[Zhibin Ren [2]]: the

删除[Zhibin Ren [2]]: ,

删除[Zhibin Ren [2]]: the

删除[Zhibin Ren [2]]: output

删除[Zhibin Ren [2]]: s

删除[Zhibin Ren [2]]: used

删除[Zhibin Ren [2]]: the

删除[Zhibin Ren [2]]: the

删除[Zhibin Ren [2]]: the

删除[Zhibin Ren [2]]: the

删除[Zhibin Ren [2]]: used

删除[Zhibin Ren [2]]: the

删除[Zhibin Ren [2]]: the

删除[Zhibin Ren [2]]: the

删除[Zhibin Ren [2]]: equation

删除[Zhibin Ren [2]]: the

删除[Zhibin Ren [2]]: power output

删除[Zhibin Ren [2]]: signal

删除[Zhibin Ren [2]]: equation

删除[Zhibin Ren [2]]: the

删除[Zhibin Ren [2]]: the

删除[Zhibin Ren [2]]: the

删除[Zhibin Ren [2]]: the

删除[Zhibin Ren [2]]: the power supply output

删除[Zhibin Ren [2]]: the

删除[Zhibin Ren [2]]: equation

删除[Zhibin Ren [2]]: through the

删除[Zhibin Ren [2]]: coaxial cable

删除[Zhibin Ren [2]]: the coaxial cable

删除[Zhibin Ren [2]]: the speed of

删除[Zhibin Ren [2]]: s

删除[Zhibin Ren [2]]: the speed of

167 4 Analysis of clock synchronization deviation

168 No matter which clock synchronization method is used, there will be a deviation between the final 1 Hz
169 square wave signal generated and the PPS from GPS. The main deviation in conventional MCSEM
170 clock synchronization method comes from the crystal oscillator inside transmitter. The generation of 1
171 Hz signal synchronized with the rising edges of PPS relies on internal crystal oscillator. If the
172 temperature drift of crystal is smaller, the frequency of output signal is more stable and the clock
173 synchronization deviation is also smaller. The clock synchronization method in this paper generates a 1
174 Hz signal synchronized to the rising edges of PPS by counting the rising edges of 400 Hz square wave.
175 Its frequency stability primarily is from the stability of 400 Hz output of power supply, reducing
176 dependence on the internal crystal oscillator. The deviation of this method comes from circuit
177 processing, cable transmission and other stages that may generate signal delay, and it can be calculated
178 by the following formula:

$$179 T = T_1 + T_2 + T_3 \quad (1)$$

180 where T is the delay of generated 1 Hz square wave signal relative to PPS, T_1 is the delay generated
181 by circuit processing stage, T_2 is the delay generated by cable transmission, T_3 is the delay caused
182 by signal passing through transformers. T_1 mainly consists of three parts: chip program processing,
183 signal transmission in all circuit, the synchronization process of power supply. T_1 can be calculated
184 by the following formula:

$$185 T_1 = T_c \times n + t_1 + t_2 \quad (2)$$

186 where T_c is the instruction cycle of chip, i.e., the time required to execute one instruction, and n is
187 the number of instructions, t_1 is the delay caused by signal transmission in all circuit, t_2 is the delay
188 generated by high-power supply synchronization output. T_c is related to the crystal oscillator used by
189 chip. In this paper, the value of T_c is 6 ns, the value of n doesn't exceed 30. t_1 is related to the
190 components used in signal transmission path in the circuit board. In this paper, the value of t_1 doesn't
191 exceed 4 ns. There is a slight delay in the zero phase of 400 Hz signal from power supply relative to the
192 rising edges of 400 Hz synchronization signal, but the power supply output signal waveform is not a
193 standard sine wave, making it difficult to precisely identify the zero phase. Therefore, it is difficult to
194 obtain an accurate result for t_2 through separate test, but subsequent overall deviation test includes t_2 .
195 T_2 mainly consists of three parts: the delay caused by coaxial cable transmission, and delay caused by
196 wires transmission between circuit boards, and it can be calculated by the following formula:

$$197 T_2 = \frac{L_{cable}}{v_{cable}} + \frac{L_{wire}}{v_{wire}} \quad (3)$$

$$198 v_{cable} = \eta_1 \times c \quad (4)$$

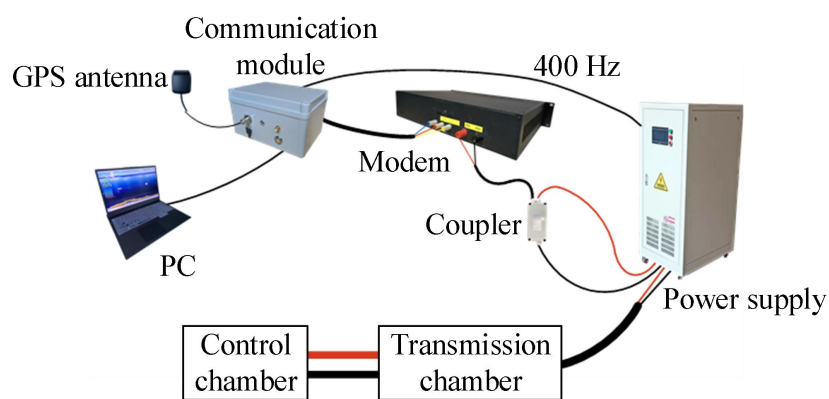
$$199 v_{wire} = \eta_2 \times c \quad (5)$$

200 where L_{cable} is the length of coaxial cable, and v_{cable} is the speed at which the signal is transmitted
201 via coaxial cable, L_{wire} is the length of wires between circuit boards, and v_{wire} is the speed at which
202 the signal is transmitted via wires, c is the speed of light in a vacuum, η_1 is the ratio of signal
203 transmission speed on coaxial cable to the speed of light in a vacuum, η_2 is the ratio of signal
204 transmission speed between circuit boards via wires to the speed of light in a vacuum. The typical value
205 of η_1 ranges from 0.67 to 0.75, and the typical value of η_2 ranges from 0.6 to 0.9 (when using
206 22AWG wire). Therefore, for every 1 km of coaxial cable, the delay typically falls within a range of
207 4.48 to 4.98 μ s. The total length of wires between circuit boards inside transmission chamber doesn't
208 exceed 1 m, resulting in a delay typically range from 3.7 to 5.56 ns.

209 The 400 Hz signal output from high-power supply passes through two stages of transformers and is
 210 reduced to low voltage ranging from 0 to 22V for processing by underwater signal processing unit. The
 211 transformers are not ideal transformers, so there is a certain phase shift between the primary input
 212 voltage and the secondary output voltage of each transformer, which is the cause of T_3 . Due to limited
 213 test condition, T_3 can't be tested separately in this paper, but subsequent overall deviation testing
 214 includes T_3 . All deviations described above can be combined and measured in the overall test of the
 215 clock synchronization method.

216 5 The test of clock synchronization method

217 In accordance with the clock synchronization method using power supply signal based on coaxial cable,
 218 as discussed in this paper, a test platform was built in laboratory to evaluate the effectiveness of clock
 219 synchronization. The test setup is shown in Fig.8. Due to the high voltage output of power supply and
 220 the low voltage requirement of modem, a coupler is needed to connect the two (Giraneza and
 221 Abo-Al-Ez, 2022; Costa et al., 2017). This coupler is a capacitive coupler, which presents significant
 222 impedance to 400 Hz AC signal. Consequently, the voltage in power carrier loop primarily accumulates
 223 at the coupler's ends. Since the frequency of power line communication exceeds 100 kHz, coupler's
 224 impedance is relatively low. Therefore, the power line communication signal can pass through coupler,
 225 but the 400 Hz synchronization signal of high-power supply does not. This coupler does not cause a
 226 delay.



227 **Fig.8** The diagram of test setup.

228
 229
 230 Fig.9 shows the clock synchronization process based on coaxial cable. First, control chamber is
 231 connected to a GPS module. Once control circuit receives PPS and records the specific timing of rising
 232 edges, GPS module is removed. Next, high power supply is activated. The 400 Hz AC signal output
 233 from power supply is converted into 1Hz square wave by the signal processing unit inside control
 234 chamber. Finally, PC sends a synchronization command and transmitter's internal clock realigns with 1
 235 Hz square wave.

删除[Zhibin Ren [2]]: the

删除[Zhibin Ren [2]]: the

删除[Zhibin Ren [2]]: the

删除[Zhibin Ren [2]]: a

删除[Zhibin Ren [2]]: a

删除[Zhibin Ren [2]]: the

删除[Zhibin Ren [2]]: the

删除[Zhibin Ren [2]]: the

删除[Zhibin Ren [2]]: The coupler used

删除[Zhibin Ren [2]]: the

删除[Zhibin Ren [2]]: the

删除[Zhibin Ren [2]]: the

删除[Zhibin Ren [2]]: the

删除[Zhibin Ren [2]]: . T

删除[Zhibin Ren [2]]: the

删除[Zhibin Ren [2]]: pass through the coupler, so the

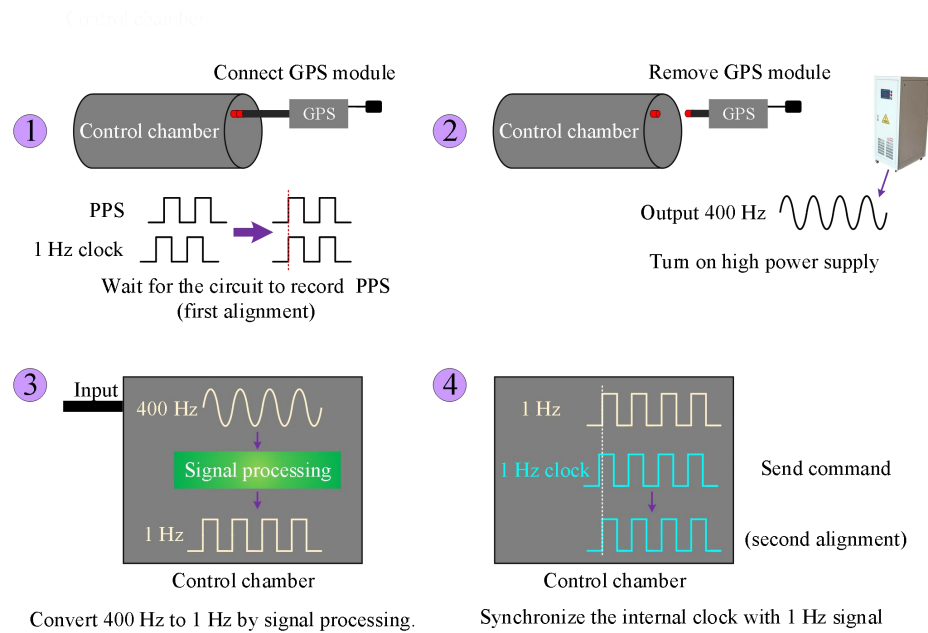


Fig.9 The clock synchronization process based on coaxial cable.

Fig.10 shows the internal clock synchronized with PPS and the clock synchronization deviation. To facilitate observation, the duty cycle of internal clock signal generated by underwater signal processing unit was set to 50%, while the duty cycle of PPS output from GPS module was set to 40%. After continuous observation, the deviation between the rising edge of internal clock signal and the rising edge of PPS was approximately 504 ns. Fig.11 presents the results of multiple tests, showing that the synchronization deviation fluctuated around 504 ns with a range of 34 ns. The coaxial cable used in test was relatively short. In marine operations, a 10 km length of coaxial cable can introduce a maximum delay of approximately 49.8 μ s. In this case, the maximum delay of internal clock signal relative to PPS would be approximately 50.3 μ s. During the measurement of internal clock signal, some interference pulses were observed, likely caused by test pins being too close to high power equipment in laboratory environment. Fig.12 shows some photos of the test scene.

Unlike Scripps transmitter, this study employs a ship-borne high-power supply to transmit 400 Hz signal and generate a 1 Hz square wave synchronized with PPS as the synchronization signal for transmitter circuit. The transmission waveform frequency control signal is generated based on the internal crystal oscillator of circuit, with its rising edge aligned with the rising edge of 1 Hz synchronization signal.

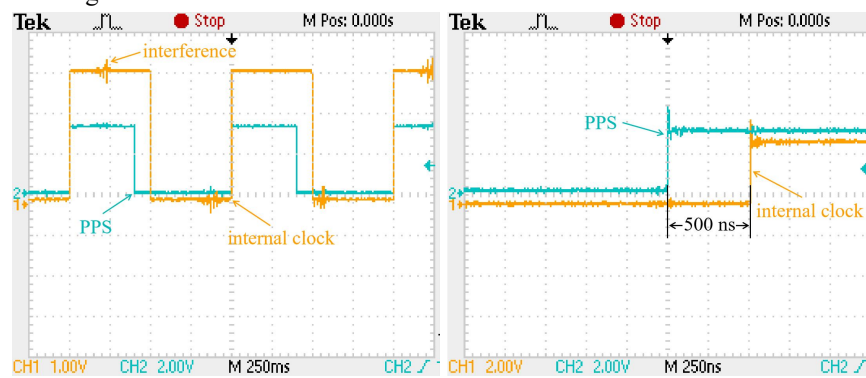


Fig.10 Internal clock synchronized with PPS (left); clock synchronization deviation (right).

删除[Zhibin Ren [2]]:
According to the predetermined operation process, the test system was powered on after the entire test system was correctly connected. Once the control circuit received the 1 Hz PPS and recorded the specific timing of the rising edges, the GPS module, which provided time to the control circuit, was removed, and the high-power supply was activated. Fig.9

删除[Zhibin Ren [2]]: the

删除[Zhibin Ren [2]]: that

删除[Zhibin Ren [2]]: the

删除[Zhibin Ren [2]]: the

删除[Zhibin Ren [2]]: the

删除[Zhibin Ren [2]]: s

删除[Zhibin Ren [2]]: the

删除[Zhibin Ren [2]]: the

删除[Zhibin Ren [2]]: include

删除[Zhibin Ren [2]]: from

删除[Zhibin Ren [2]]: a

删除[Zhibin Ren [2]]: the

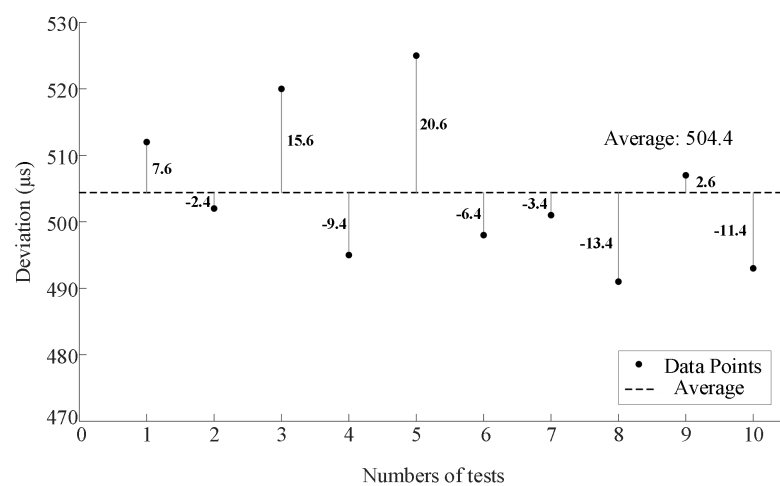
删除[Zhibin Ren [2]]: the

删除[Zhibin Ren [2]]: the

删除[Zhibin Ren [2]]: the

删除[Zhibin Ren [2]]: 9

257



258

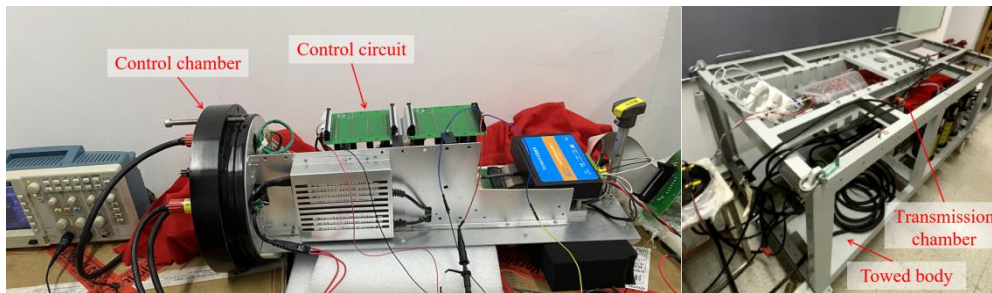
259

260

261

Fig.11 The graph of multiple tests results for synchronization deviation, shows the difference between each result and the average value.

删除[Zhibin Ren [2]]: 10



262

263

264

Fig.12 Control chamber (left); transmission chamber (right).

删除[Zhibin Ren [2]]: 11

6 Conclusion

This paper introduces a clock synchronization method of marine controlled source electromagnetic transmitter base on coaxial cable and builds related hardware system. In this method, the ship-borne high power-supply outputs 400 Hz signal synchronized with PPS, and transmits it to underwater transmitter. The transmitter control circuit can generates a 1 Hz square wave signal synchronized with PPS for clock synchronization. The delay deviation of 1 Hz square wave signal obtained by this method relative to PPS is less than 1 ms, which meets the requirement of synchronization accuracy better than 1 ms in practical operations and can be used for internal clock synchronization of transmitter. This method can facilitate the use of coaxial cables in MCSEM operations, and expand transmitter's application scenarios. This method can also provide a reference for the design of other underwater equipment that uses coaxial cables.

7 Statement

This manuscript satisfies the following statements that: 1) all authors agree with the submission, 2) the work has not been published elsewhere, either completely, in part, or in another form, and 3) the manuscript has not been submitted to another journal.

Data availability

No data sets were used in this article.

Author contributions

M. Wang is the project applicant and a key participant in the testing process. K. Chen provided some

删除[Zhibin Ren [2]]: the

删除[Zhibin Ren [2]]: the

删除[Zhibin Ren [2]]: the

删除[Zhibin Ren [2]]: the rising edges of the

删除[Zhibin Ren [2]]: the rising edges of

删除[Zhibin Ren [2]]: for clock synchronization accuracy of better than 1ms

删除[Zhibin Ren [2]]: the

删除[Zhibin Ren [2]]: This method has a positive effect on the future operation of marine controlled source electromagnetic transmitters carrying more ships.

284 optimization suggestions for the test scheme. C.T. Wang and R.Y. Yu, as the research assistants, had
285 helped complete the testing. Z.B. Ren is the project leader, primarily responsible for the test scheme
286 design, hardware circuit design, and other related tasks.

287 **Competing interests**

288 The contact author has declared that none of the authors has any competing interests.

289 **Financial support**

290 This work was supported by the National Natural Science Foundation of China (42374221), the Key
291 Technologies R&D Program (2022YFC2807900), Marine Economic Development in Guangdong
292 Province (Grant Number: GDNRC[2023]40).

293 **Acknowledgement**

294 Thanks to the editors and reviewers. Additionally, this paper was supported by south China sea institute
295 of oceanology, cas and Fujian earthquake agency. The authors express thanks to the two mentioned
296 institutions.

297 **References**

- 298 Amuta, E., Awelewa, A., Olajube, A., Somefun, T., Afolabi, G., and Uyi, A.: Power line carrier
299 technologies: a review, IOP Conference Series: Materials Science and Engineering, Ota, Nigeria,
300 27th-28th July 2020, 012062, doi: 10.1088/1757-899X/1036/1/012062, 2021.
- 301 Chen, K., Deng, M., Wu, Z., Jing, J., Luo, X., and Wang, M.: Low Time Drift Technology for Marine
302 CSEM Recorder, *Geoscience*, 26, 1312-1316, doi: 10.3969/j.issn.1000-8527.2012.06.027, 2012.
- 303 Chen, K., Deng, M., Yu, P., Yang, Q., Luo, X. H., and Yi, X. P.: A near-seafloor-towed CSEM receiver
304 for deeper target prospecting, *Terrestrial Atmospheric and Oceanic Sciences*, 31, 565-577, doi:
305 10.3319/tao.2020.08.03.01, 2020.
- 306 Constable, S.: Marine electromagnetic methods—A new tool for offshore exploration, *The Leading*
307 *Edge*, 25, 438-444, doi: 10.1190/1.2193225, 2006.
- 308 Constable, S.: Ten years of marine CSEM for hydrocarbon exploration, *Geophysics*, 75, 75A67-75A81,
309 doi: 10.1190/1.3483451, 2010.
- 310 Constable, S.: Review paper: Instrumentation for marine magnetotelluric and controlled source
311 electromagnetic sounding, *Geophysical Prospecting*, 61, 505-532, doi:
312 10.1111/j.1365-2478.2012.01117.x, 2013.
- 313 Constable, S. and Srnka, L. J.: An introduction to marine controlled-source electromagnetic methods
314 for hydrocarbon exploration, *Geophysics*, 72, WA3-WA12, doi: 10.1190/1.2432483, 2007.
- 315 Costa, L. G. d. S., Queiroz, A. C. M. d., Adebisi, B., Costa, V. L. R. d., and Ribeiro, M. V.: Coupling for
316 power line communications: A survey, *Journal of Communication and Information Systems*, 32, doi:
317 10.14209/jcis.2017.2, 2017.
- 318 Cox, C., Constable, S., Chave, A., and Webb, S.: Controlled-source electromagnetic sounding of the
319 oceanic lithosphere, *Nature*, 320, 52-54, doi: 10.1038/320052a0, 1986.
- 320 Edwards, R. and Chave, A.: A transient electric dipole-dipole method for mapping the conductivity of
321 the sea floor, *Geophysics*, 51, 984-987, doi: 10.1190/1.1442156, 1986.
- 322 Ferreira, H. C., Grové, H. M., Hooijen, O., and Vinck, A. H.: Power line communication, *Wiley*
323 *Encyclopedia of Electrical and Electronics Engineering*, 16, 706-716, doi:
324 10.1002/047134608X.W2004, 2001.
- 325 Giraneza, M. and Abo-Al-Ez, K.: Power line communication: A review on couplers and channel
326 characterization, *AIMS Electronics and Electrical Engineering*, 6, 265-284, doi:
327 10.3934/electreng.2022016, 2022.

328 Kaddoum, G. and Tadayon, N.: Differential chaos shift keying: A robust modulation scheme for
329 power-line communications, *IEEE Transactions on Circuits and Systems II: Express Briefs*, 64, 31-35,
330 doi: 10.1109/TCSII.2016.2546901, 2016.

331 Liu, Y., Yin, C., Weng, A., and Jia, D.: Attitude effect for marine CSEM system, *Chinese Journal of*
332 *Geophysics*, 55, 2757-2768, doi: 10.6038/j.issn.0001-5733.2012.08.027, 2012.

333 Meng, W., Ming, D., Qi-sheng, Z., Kai, C., and Jin-ling, C. U. I.: The technique of time
334 synchronization operation to control marine electromagnetic emission, *Progress in Geophysics*, 24,
335 1493-1498, doi: 10.3969/j.issn.1004-2903.2009.04.043, 2009.

336 Qiu, Y., Yang, Q., Deng, M., and Chen, K.: Time synchronization and data transfer method for towed
337 electromagnetic receiver, *Review of Scientific Instruments*, 91, doi: 10.1063/5.0012218, 2020.

338 Wang, M., Deng, M., Zhao, Q., Luo, X., and Jing, J.: Two types of marine controlled source
339 electromagnetic transmitters, *Geophysical Prospecting*, 63, 1403-1419, doi: 10.1111/1365-2478.12329,
340 2015a.

341 WANG, M., DENG, M., WU, Z.-L., LUO, X.-H., JING, J.-E., and CHEN, K.: New type deployed
342 marine controlled source electromagnetic transmitter system and its experiment application, *Chinese*
343 *Journal of Geophysics*, 60, 4253-4261, doi: 10.1111/1365-2478.12329, 2017a.

344 Wang, M., Deng, M., Wu, Z., Luo, X., Jing, J., and Chen, K.: The deep-tow marine controlled-source
345 electromagnetic transmitter system for gas hydrate exploration, *Journal of Applied Geophysics*, 137,
346 138-144, doi: 10.1016/j.jappgeo.2016.12.019, 2017b.

347 WANG, M., WU, Z.-l., DENG, M., MA, C.-w., LIU, Y., and WANG, S.-x.: The high precision time
348 stamp technology in MCSEM transmission current waveform, *Progress in Geophysics*, 30, 1912-1917,
349 doi: 10.6038/pg20150452, 2015b.

350 Wang, M., Zhang, H.-Q., Wu, Z.-L., Sheng, Y., Luo, X.-H., Jing, J.-E., and Chen, K.: Marine controlled
351 source electromagnetic launch system for natural gas hydrate resource exploration, *Chinese Journal of*
352 *Geophysics*, 56, 3708-3717, doi: 10.6038/cjg20131112, 2013.

353 Wang, M., Ming, D., Li, X., Zhang, Z., Yue, H., Zhang, T., Duan, N., and Ma, X.: The latest
354 development of Marine controllable source electromagnetic transmitter, *IOP Conference Series: Earth*
355 *and Environmental Science*, Changchun, China, 11-14 October 2020, 012137, doi:
356 10.1088/1755-1315/660/1/012137, 2021.

357